



Present status of PNPI-ILL EDM experiment

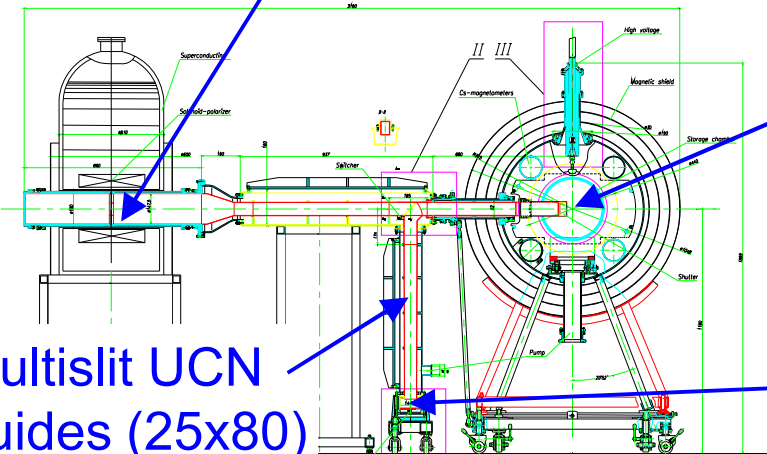
1. Sensitivity determination of multi-chamber EDM spectrometer and double-chamber EDM spectrometer
2. First scientific results: new constraints for CP-violating long-range forces

A.P. Serebrov

7th UCN Workshop
“Ultra Cold & Cold Neutrons
Physics & Sources”
8-14 June 2009

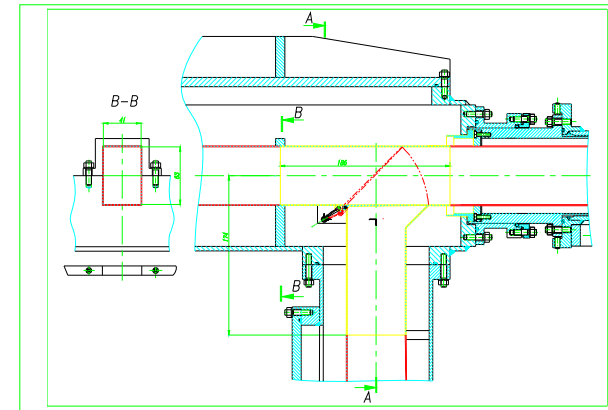
Scheme of multi-chamber EDM spectrometer (test model)

high polished cylindrical UCN guide ($\varnothing 120$) with $^{58}\text{NiMo}$ coating



BeO coated traps,
Be coated electrodes

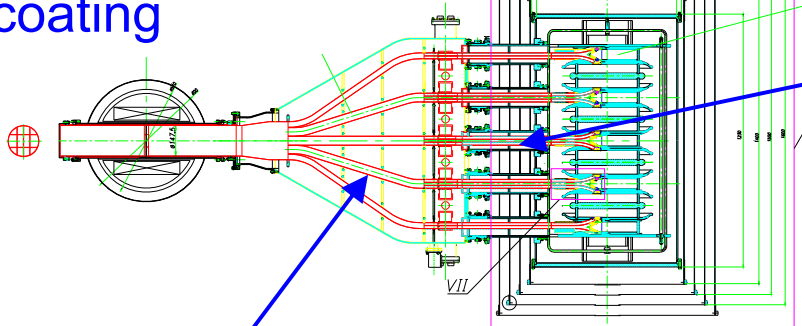
shutter system



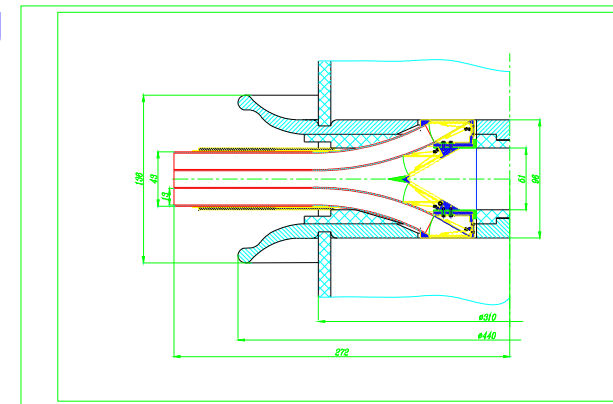
multislit UCN guides (25x80) with $^{58}\text{NiMo}$ coating

Si-UCN detectors with ^6LiF coating

distributing valves



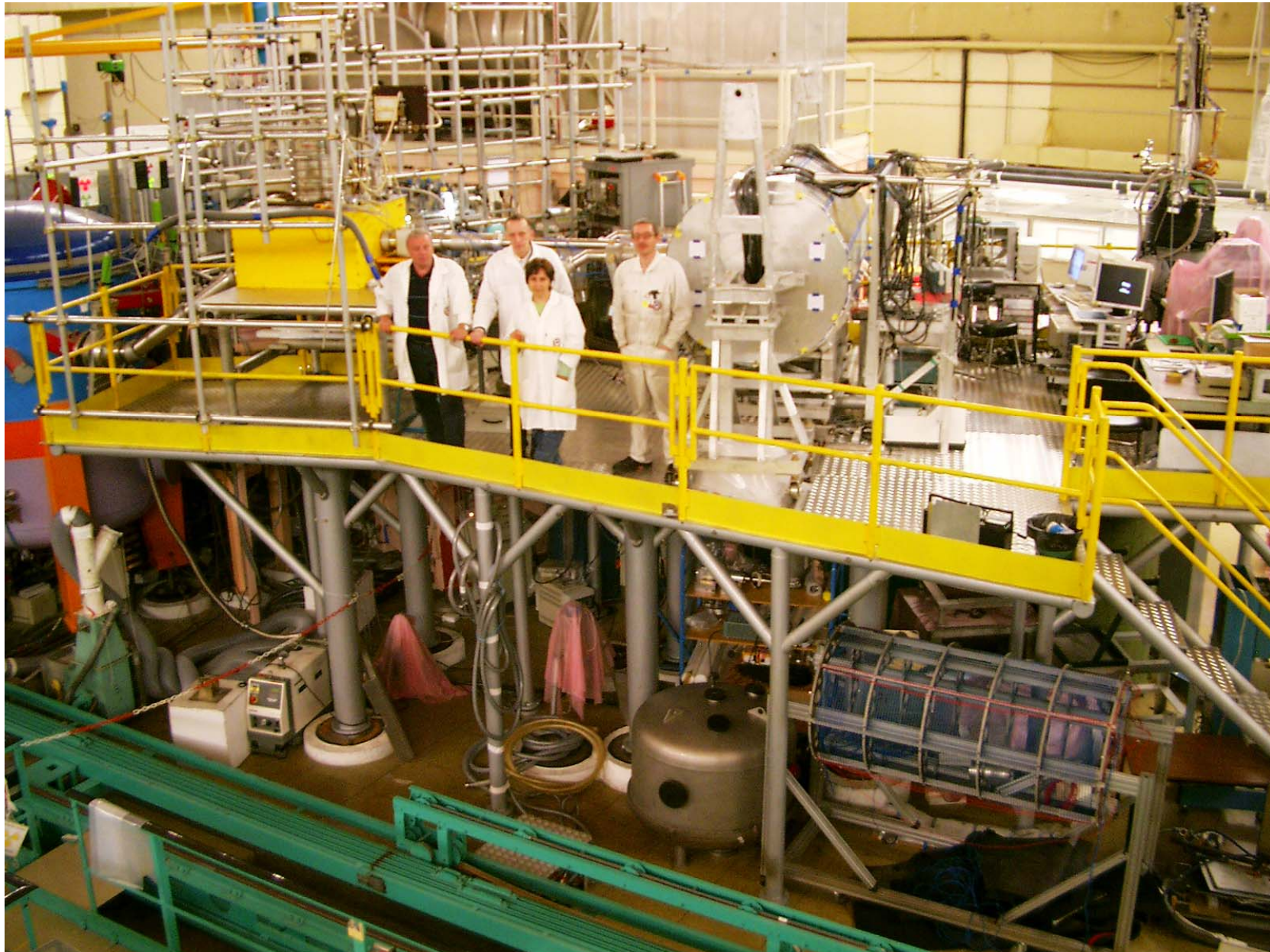
multislit UCN guides (25x80) with Be coating



rectangular UCN guides (80x80) with Be coating

trap valves

December 2007. Assembly of multi-chamber EDM spectrometer



December 2007. Assembly of multi-chamber EDM spectrometer



Assembly of multi-chamber trap



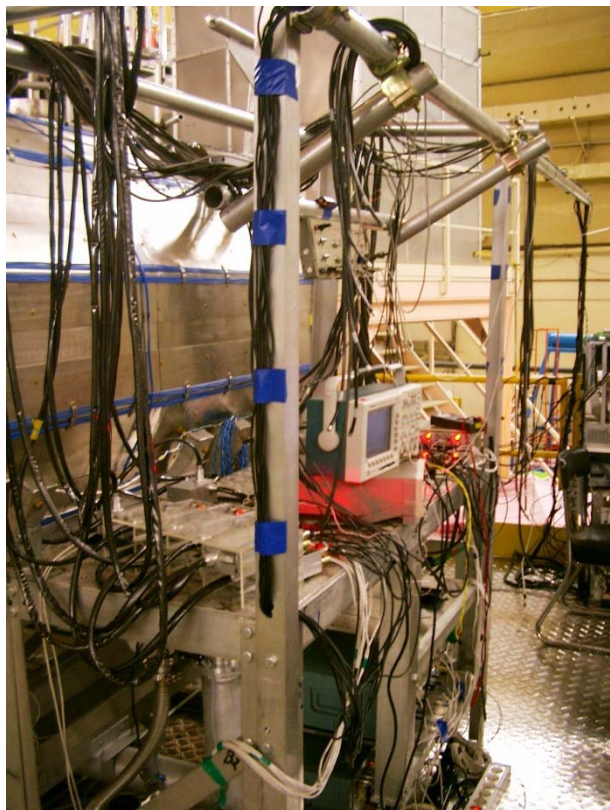
UCN detector with analysis of polarization
(13 neutron channels, 117 Si detectors with electronics)

**December 2007. Assembly of neutron guide system and switcher.
March 2008. Reparation of switcher and UCN guides**

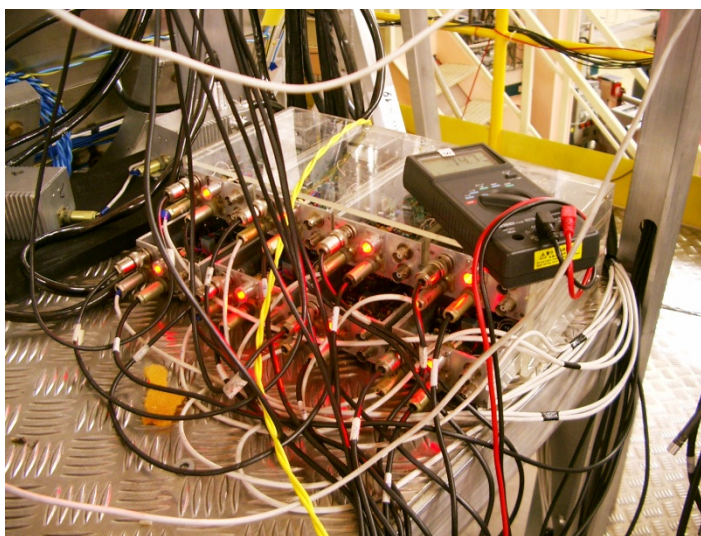
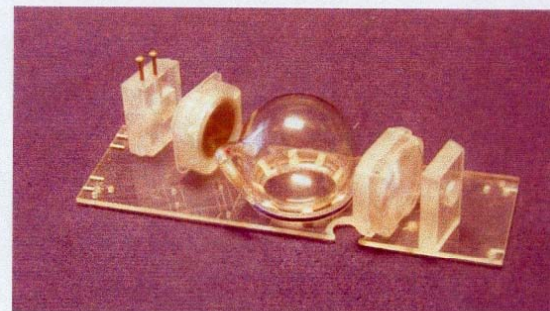
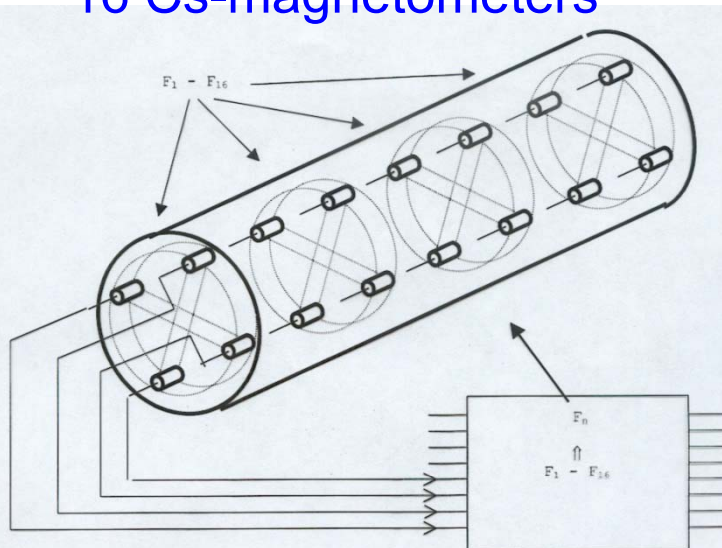


Neutron guide system and switcher

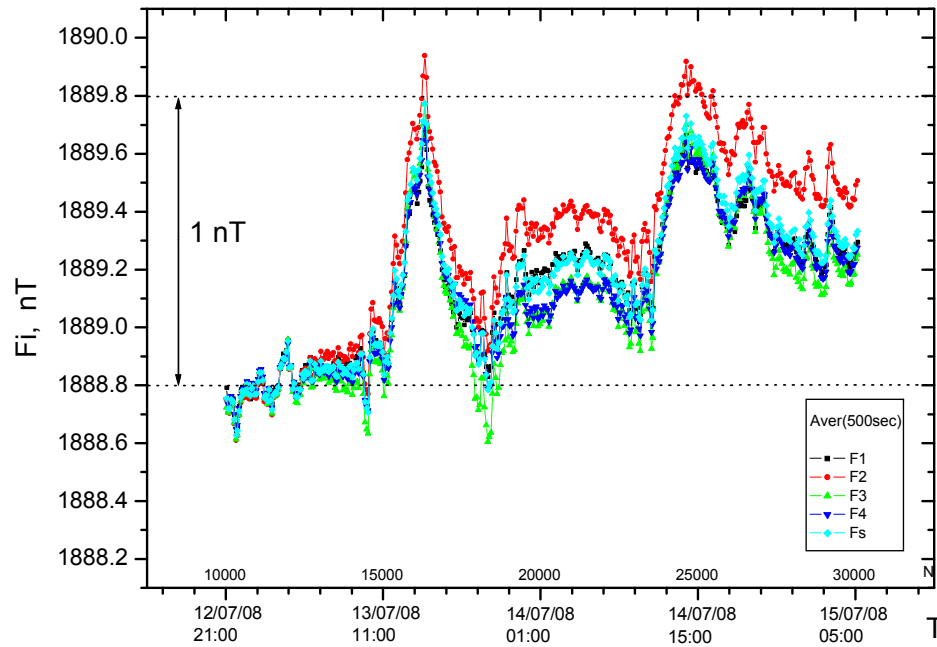
System of 16 Cs-magnetometers



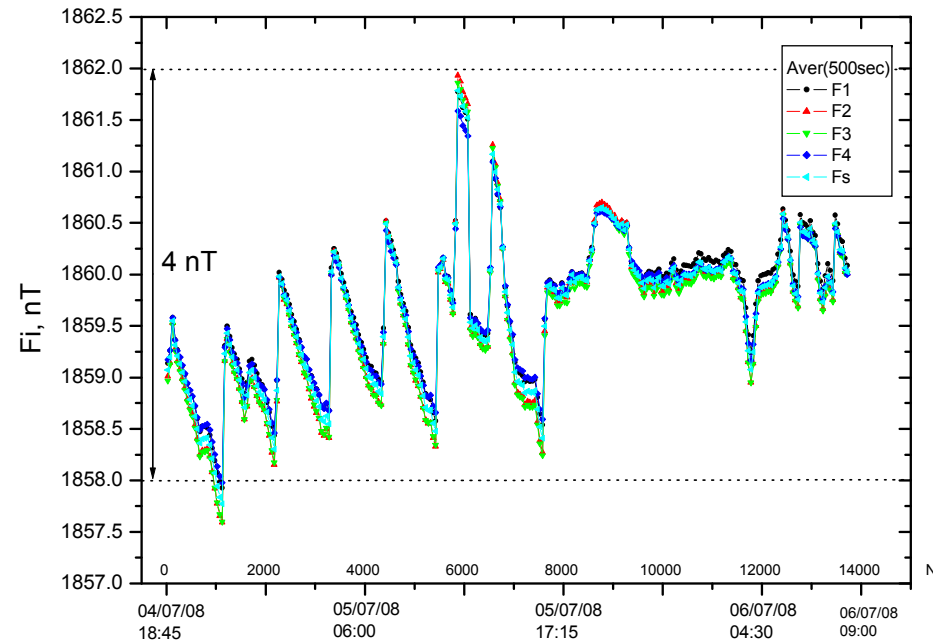
The scheme of 16 Cs-magnetometers



Magnetic field of multi-chamber EDM spectrometer

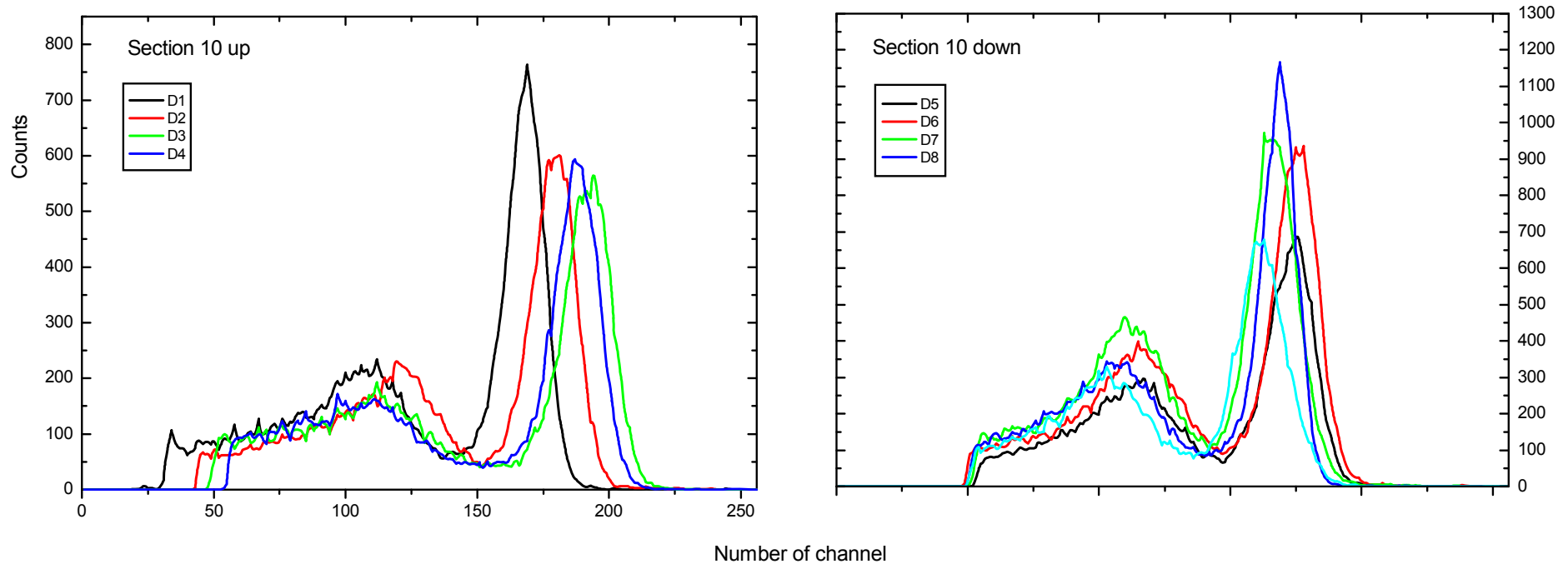


“Typical” drifts of the magnetic field inside the spectrometer



“Extreme” drifts of the magnetic field inside the spectrometer

UCN detector system (13 neutron channels, 117 Si detectors)



Left: pulse height spectra of upper part of detector array 10 placed above analyzer foil and consisting of 4 detectors with size 2 cm x 6 cm. Right: spectra of lower part of detector array placed under analyzing foil and consisting of 5 detectors with sizes 2 cm x 6 cm.

Preliminary estimation of sensitivity of multi-chamber EDM spectrometer

Number of UCN captured in the traps:

$$N=5.1 \cdot 10^4 \quad (\rho=0.85 \text{ n/cm}^3)$$

Storage time in the traps:

$$\tau_{\text{stor}}=47 \text{ s}$$

Estimation of sensitivity:

$$1.5 \cdot 10^{-25} \text{ e}\cdot\text{cm/day}$$

Unfortunately, UCN density is about 4 times less than expected.

Problems of multi-chamber EDM spectrometer

1. Noise of Si-detector (complicated electronic system).

Improvement of UCN detector system is required!

2. Two double-chamber scheme with three monitor chambers is optimal one.
3. In the middle of 2nd reactor cycle 2008 we revealed the damage of the electric contact of the current input inside the cryostat of the superconducting UCN polarizer.

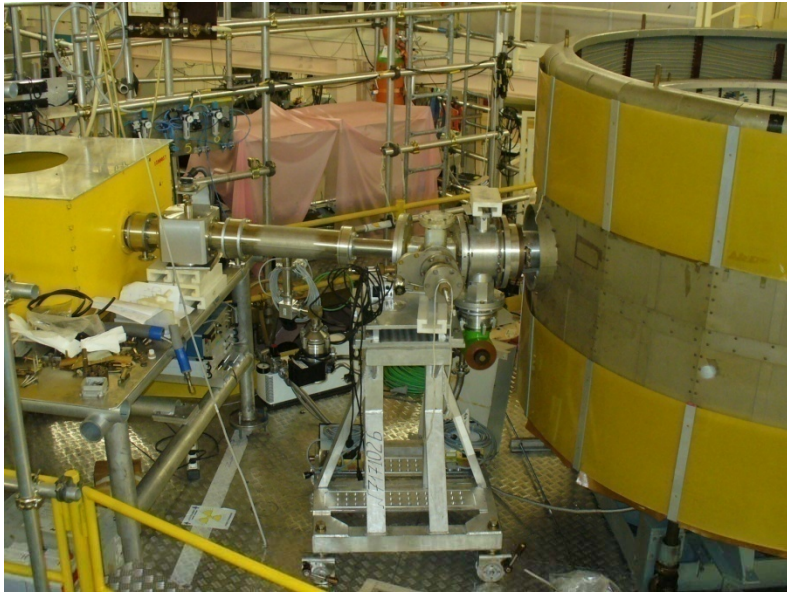
The complicated reparation has to be done!

We were forced to continue program by means old double-chamber EDM spectrometer.

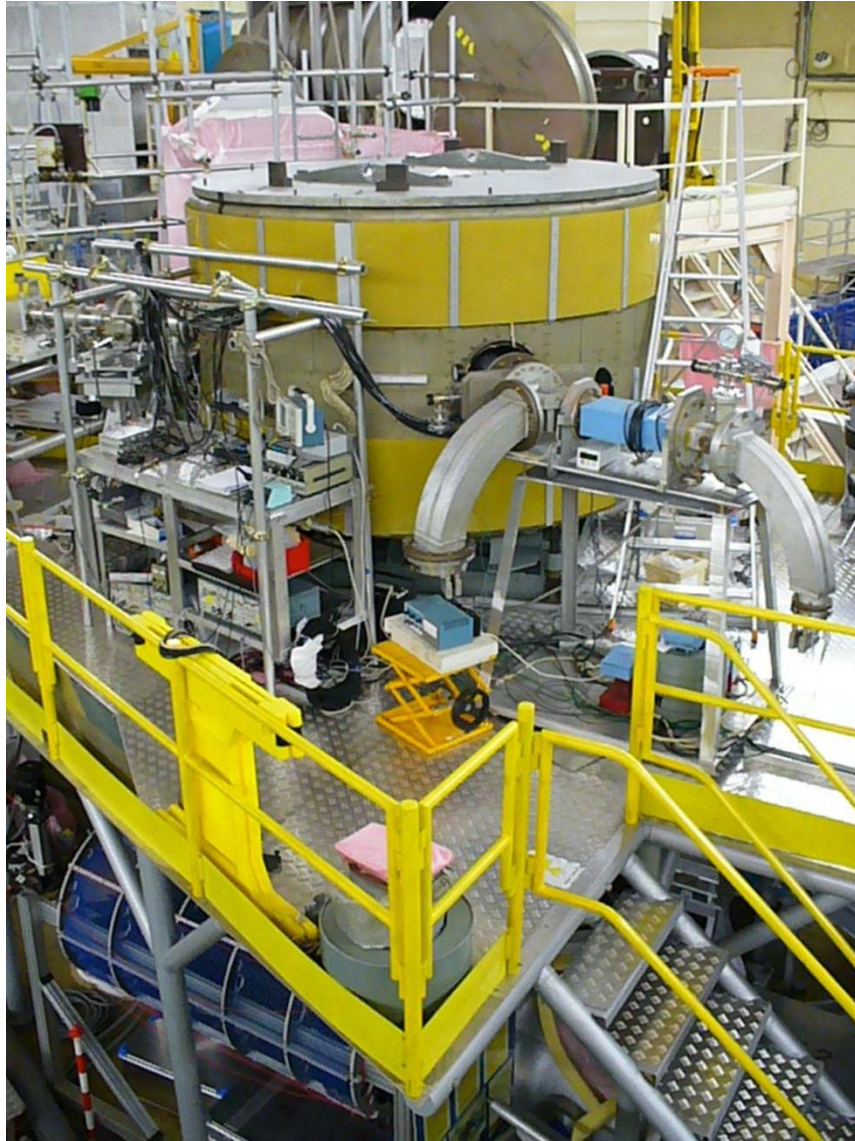
Assembly of double-chamber EDM spectrometer in summer 2008 in the interval between reactor cycles



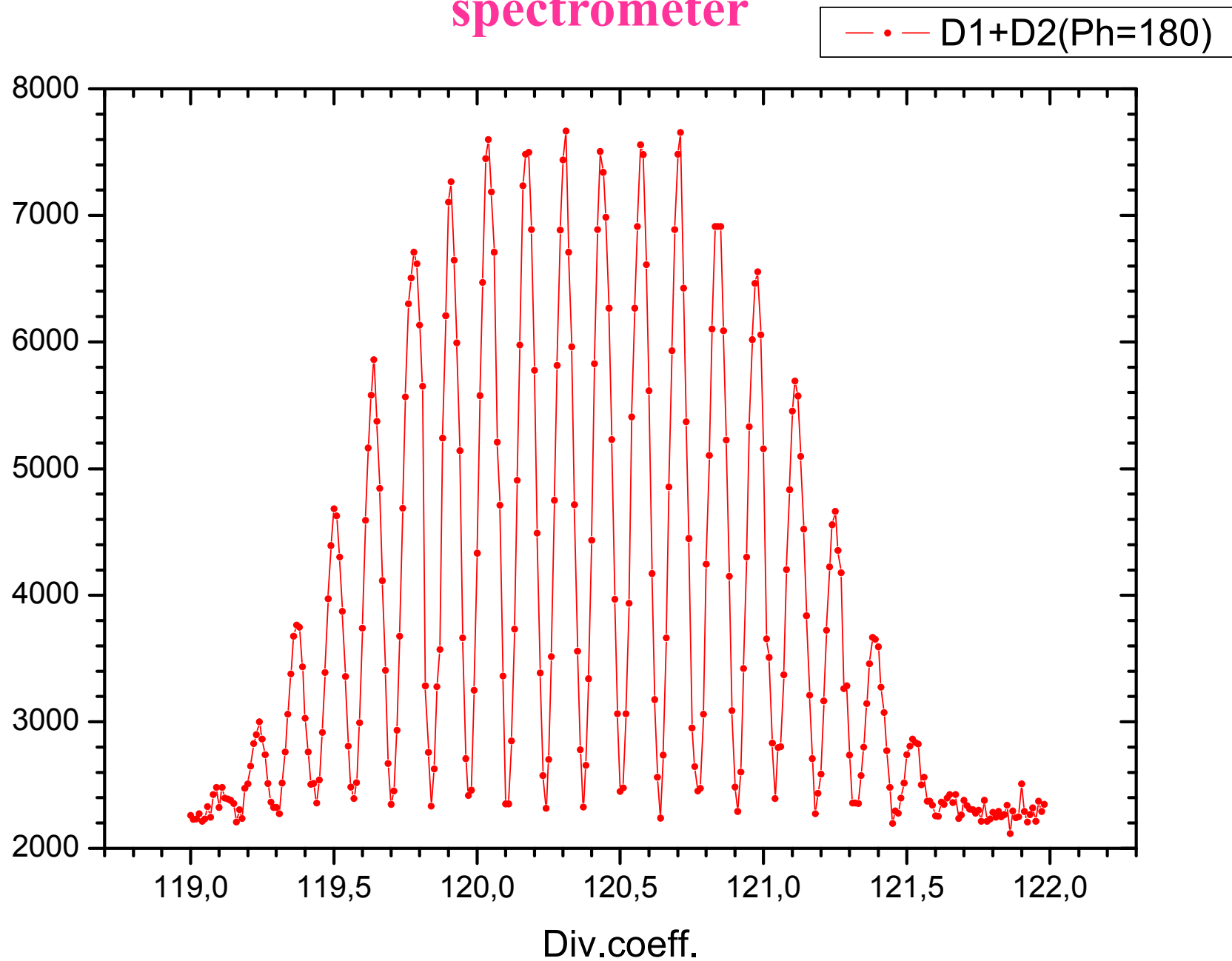
August 2008. Completion of main part of assembly.



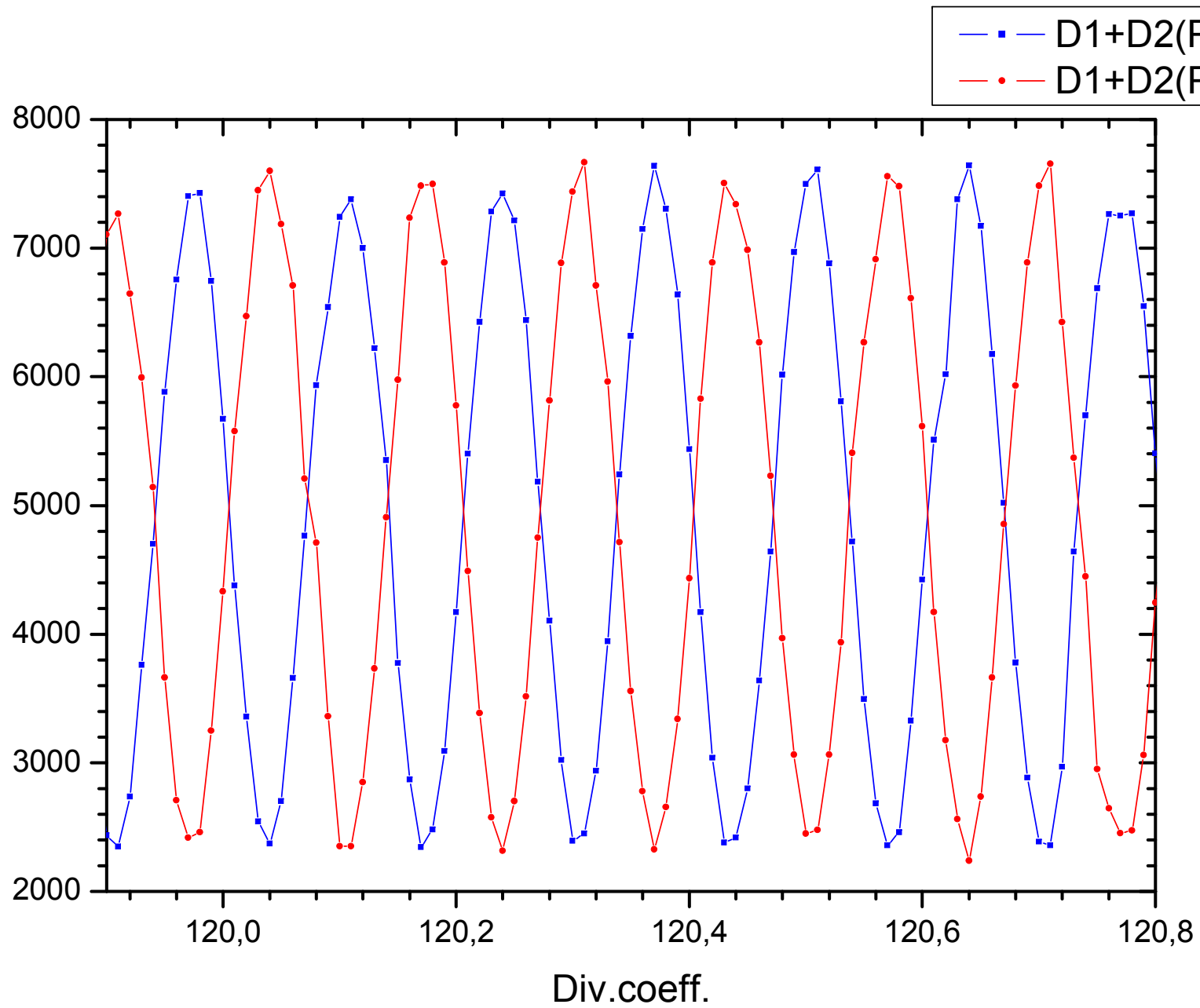
September 2008. Start of the first measurements



Resonance curve of the double-chamber EDM spectrometer

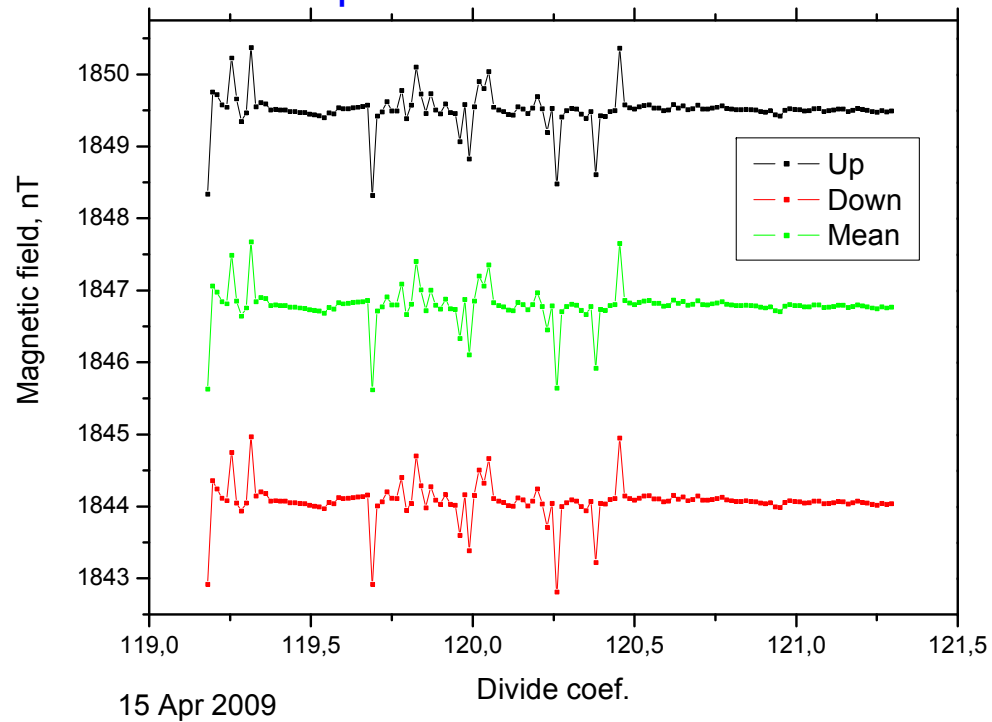


Resonance curve of the double-chamber EDM spectrometer

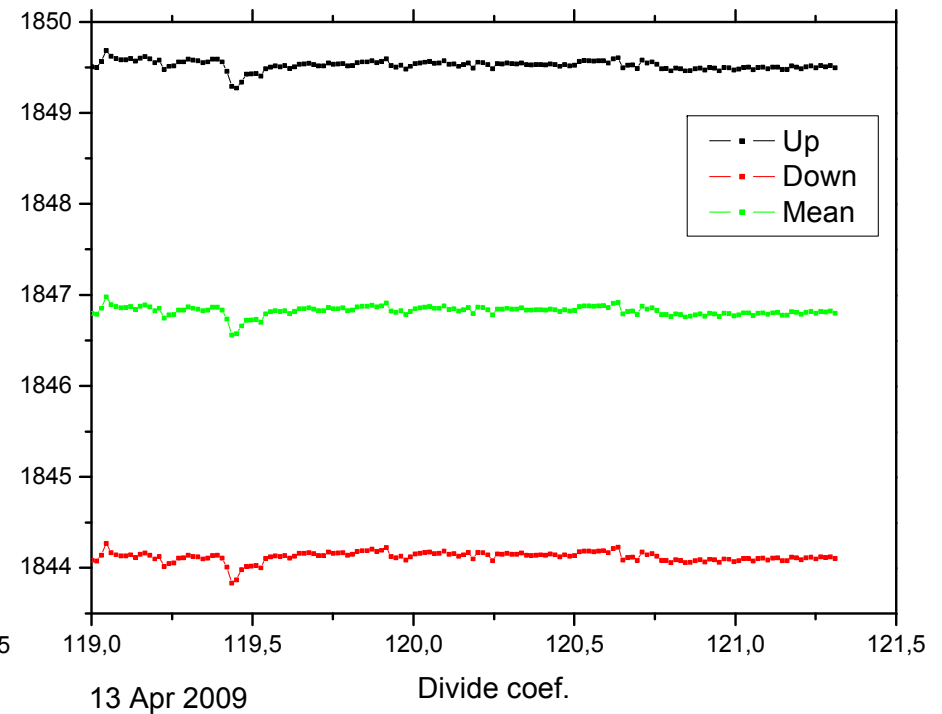


Stability of magnetic field during resonance measurements (system of stabilization of resonance conditions + feedback by means current coils)

full day tests of bridge crane
after reparation



quiet magnetic situation



Preliminary estimation of sensitivity of double-chamber EDM spectrometer

Number of UCN captured in the spectrometer trap:

$$N=4.1 \cdot 10^4$$

Storage time:

$$\tau_{\text{stor}}=55 \text{ s}$$

Sensitivity:

$$1.5 \cdot 10^{-25} \text{ e} \cdot \text{cm}/\text{day}$$

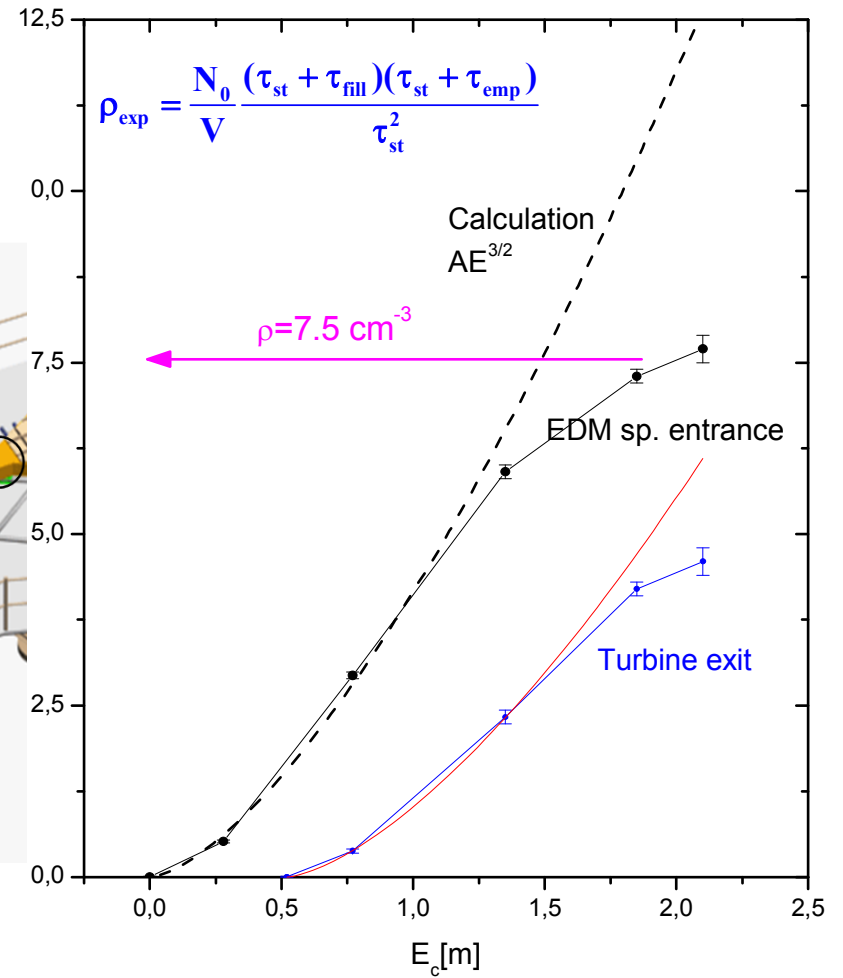
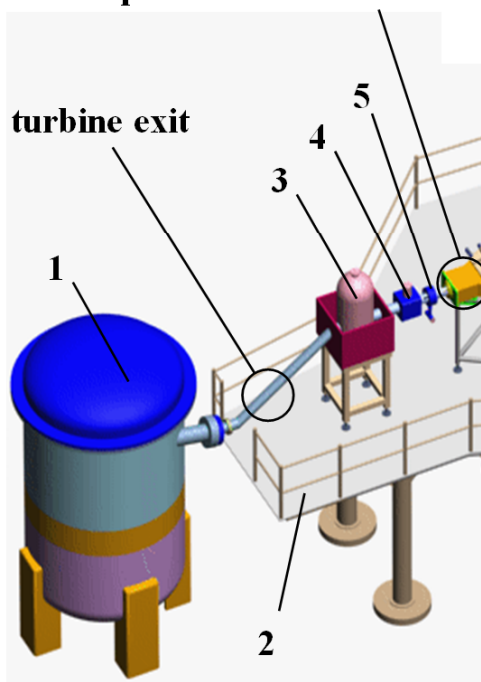
Unfortunately, UCN density in the traps again about $1 \text{ n}/\text{cm}^3$.

Direct measurements of UCN density in the EDM spectrometer entrance and at the UCN turbine exit



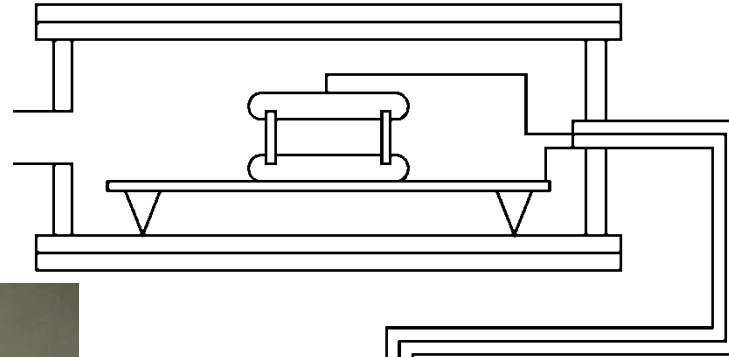
EDM spectrometer entrance

turbine exit

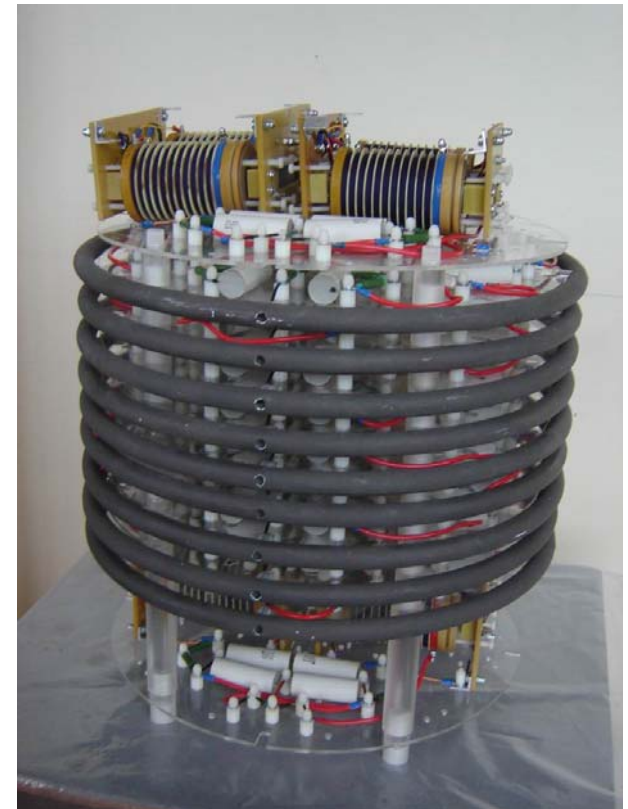
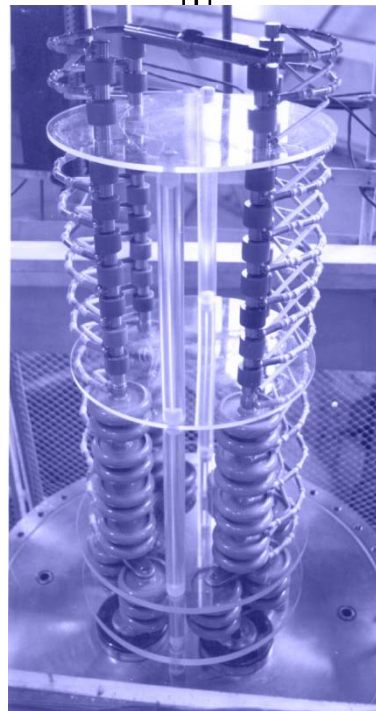


High-voltage test in PNPI (30 kV/cm – 5 cm, 20 kV/cm – 8 cm)

vacuum vessel of
new device



new HV device
with changeable
polarity



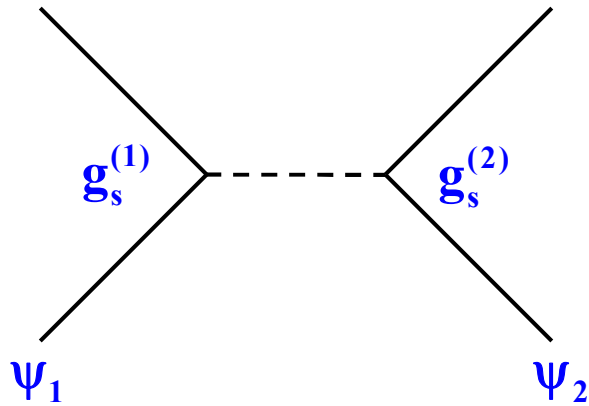
Conclusion *(for the 1st part)*

To reach accuracy of measurements $1 \cdot 10^{-26}$ e·cm
(three times better than present limit $3 \cdot 10^{-26}$ e·cm)
2 years of measurements are required.

2. New constraints for CP-violating forces in range 10^{-4} cm – 1 cm

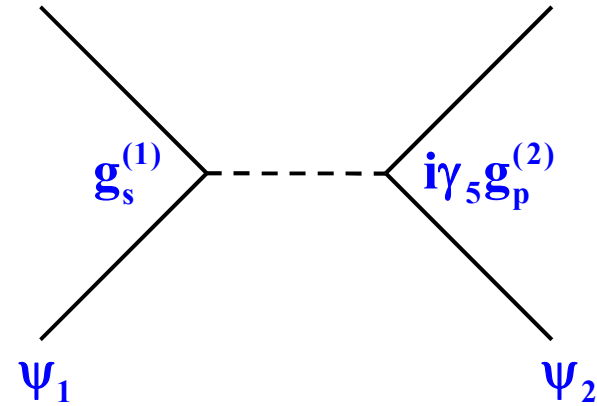
Possible long-range interaction (axion-like interaction) between nucleons

A.A. Anselm JETP Lett.
v36 N2 (1982)



$$V(\mathbf{r}) = -\frac{\mathbf{g}_s^{(1)} \mathbf{g}_s^{(2)}}{4\pi r} e^{-\frac{r}{\lambda}}$$

J.E. Moody and Frank Wilczek
Phys. Rev. D v30 N1 (1984)



$$V(\mathbf{r}) = \mathbf{g}_s^{(1)} \mathbf{g}_p^{(2)} \frac{\vec{\sigma}_2 \vec{r}}{8\pi M_2} \left[\frac{1}{r\lambda} + \frac{1}{r^2} \right] e^{-\frac{r}{\lambda}}$$

Direct experimental limits for $g_S g_P$ and “axion window” of mass or distance of interaction

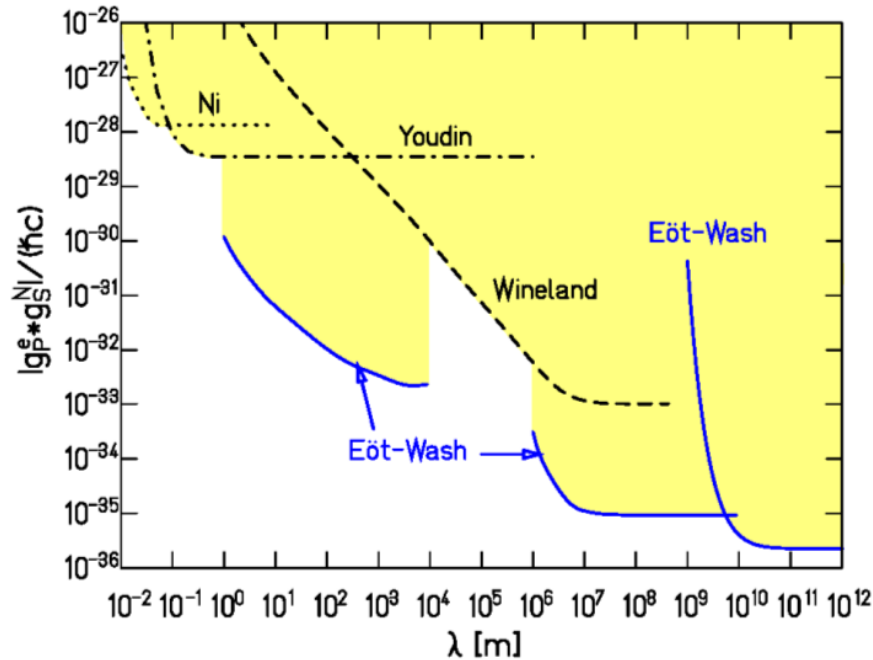


Figure 1: Short-distance gravity upper limits [37] on the product of mass- and spin-vertex couplings as a function of the interaction range λ ; the shaded region is excluded at 95% confidence. Figure courtesy E. Adelberger.

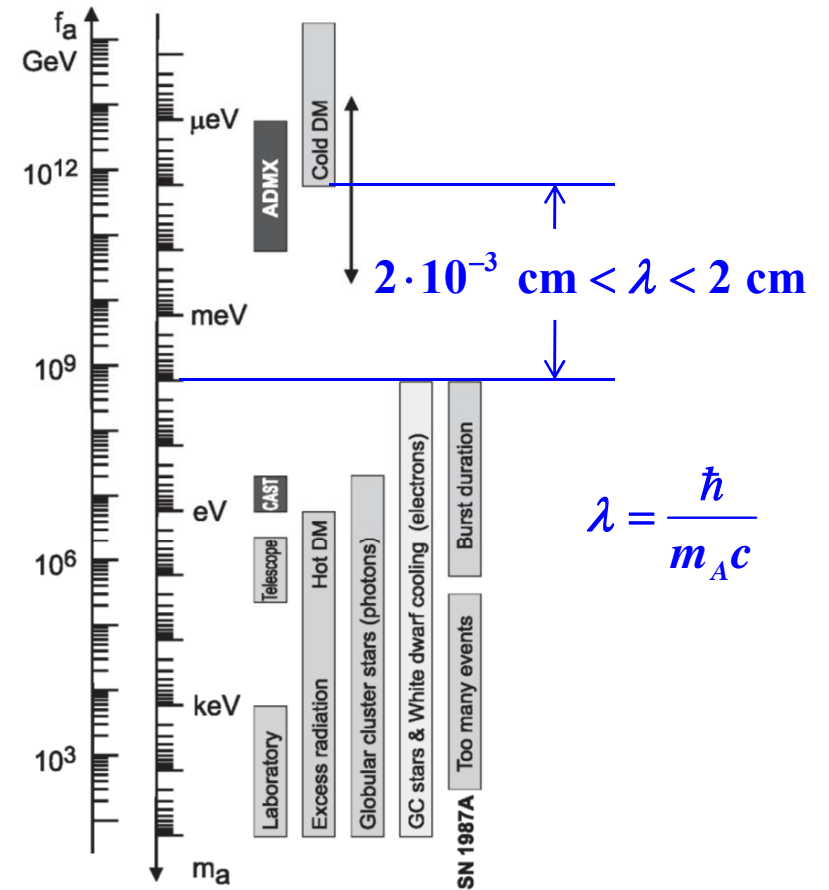


Figure 2: Exclusion and experimental search ranges as described in the text. Limits on coupling strengths are translated into limits on m_A and f_A using $z = 0.56$ and the KSVZ values for the coupling strengths. The “Laboratory” bar is a rough representation of the exclusion range for standard or variant axions. The “GC stars and white-dwarf cooling” range uses the DFSZ model with an axion-electron coupling corresponding to $\cos^2 \beta = 1/2$. The Cold Dark Matter exclusion range is particularly uncertain. We show the benchmark case from the misalignment mechanism.

Additional potential near material surface

$$V(\mathbf{r}) = g_s g_p \frac{\boldsymbol{\sigma} \cdot \mathbf{n}}{8\pi m_n} \left(\frac{1}{\lambda r} + \frac{1}{r^2} \right) e^{-r/\lambda}$$

$$V(z) = \pm V_0 e^{-z/\lambda} \left(1 - e^{-d/\lambda} \right) \Big|_{d \gg \lambda} \approx \pm V_0 e^{-z/\lambda}$$

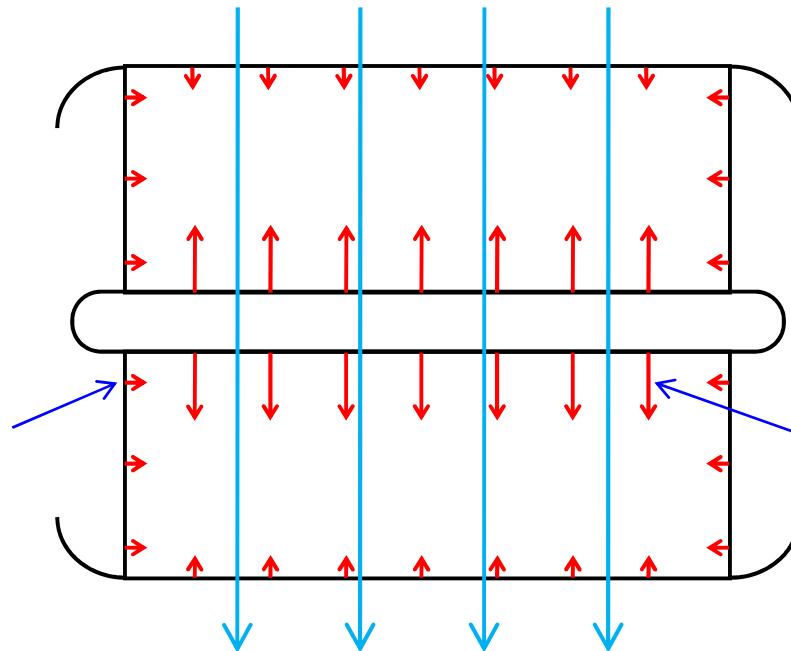
where $V_0 = \frac{\hbar^2 \lambda}{4m_n \mu_n} N g_s g_p$

Additional effective magnetic field in EDM spectrometer

$$V(z) = \pm 5.2 \cdot 10^5 [\text{eV} / \text{cm}] \lambda [\text{cm}] e^{-\frac{z}{\lambda}} g_S g_P = \pm \mu_n H_{\text{eff}} \quad \mu_n = 6 \cdot 10^{-12} [\text{eV} / \text{G}]$$

$$H_{\text{eff}} = \frac{5.2 \cdot 10^5 \lambda e^{-\frac{z}{\lambda}} g_S g_P}{\mu_n} = 8.7 \cdot 10^{16} [\text{G} / \text{cm}] \lambda [\text{cm}] g_S g_P e^{-\frac{z}{\lambda}}$$

UCN depolarization
on vertical walls
A. Serebrov
(arxiv:0902.1056)



shift of resonances
on horizontal walls
O. Zimmer
(arxiv:0810.3215)

Calculation of UCN depolarization per one wall collision

The pseudo-magnetic field near to a surface is described by dependence:

$$\mathbf{H}(\mathbf{r}) = \mathbf{H}_{r_0}(\lambda) e^{-|\mathbf{r}-\mathbf{r}_0|/\lambda}$$

where

$$\mathbf{H}_{r_0} = \frac{\hbar^2 \lambda}{4m_n \mu_n} N \mathbf{g}_S \mathbf{g}_P$$

In system of coordinates of a moving neutron $\mathbf{H}(\mathbf{r})$ is transformed to $\mathbf{H}_r(t)$:

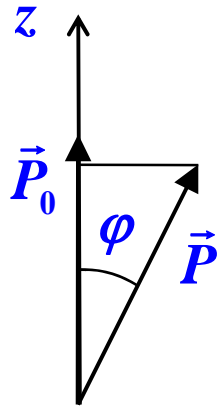
$$\mathbf{H}_r(t) = \mathbf{H}_{r_0}(\lambda) e^{-|t|/\tau_\lambda}$$

where $\tau_\lambda = \lambda / v_n$, v_n - normal component of speed to a wall surface.

Thus, in rotating system of coordinates of a moving neutron:

$$\mathbf{H}(t) = \mathbf{H}_{r_0}(\lambda) e^{-|t|/\tau_\lambda} \cos \omega_z t$$

Calculation of UCN depolarization per one wall collision



$$P_z = P_0 \cos \varphi \approx P_0 \left(1 - \varphi^2 / 2\right)$$

$\beta = \varphi^2 / 2$ - probability of depolarization for one wall collision

$$\varphi = 2\pi\gamma H_{r_0} \int_{-\infty}^{+\infty} e^{-|t|/\tau_\lambda} \cos \omega_z t dt = \frac{4\pi\gamma H_{r_0} \tau_\lambda}{1 + (\omega_z \tau_\lambda)^2}$$

$$\varphi = \frac{2\omega_\lambda \tau_\lambda}{1 + (\omega_z \tau_\lambda)^2}$$

where $\omega_\lambda = 2\pi\gamma H_{r_0} (\lambda)$

$$\beta = \frac{1}{2} \left[\frac{2\omega_\lambda \tau_\lambda}{1 + (\omega_z \tau_\lambda)^2} \right]^2$$

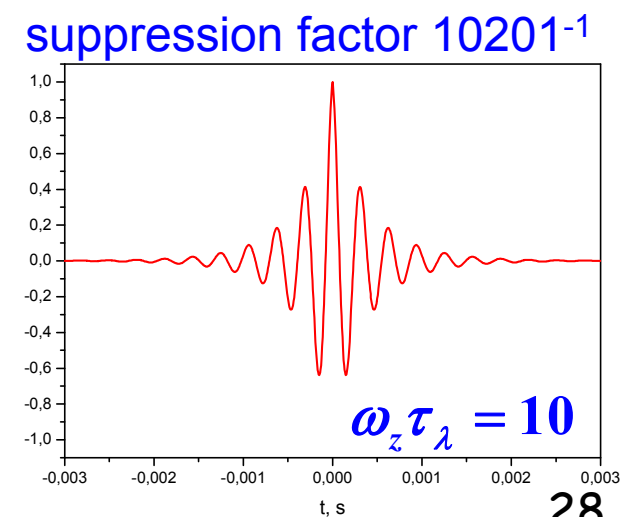
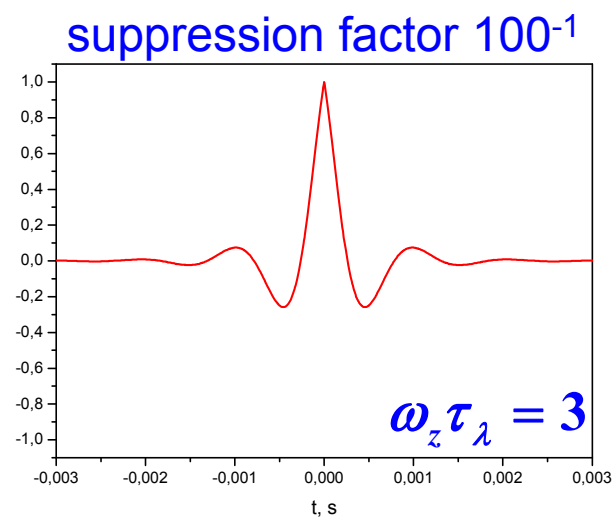
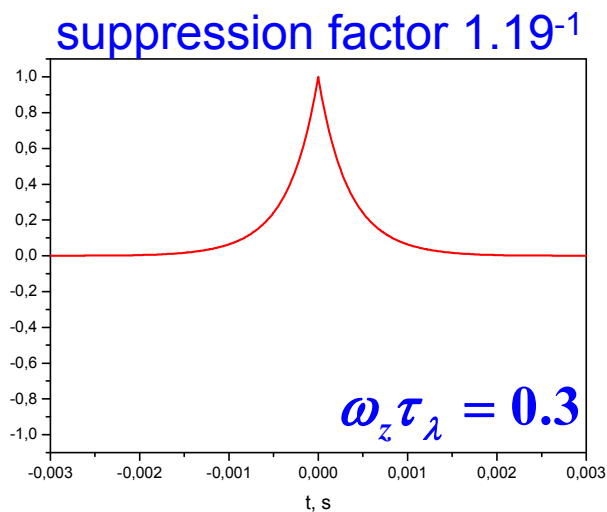
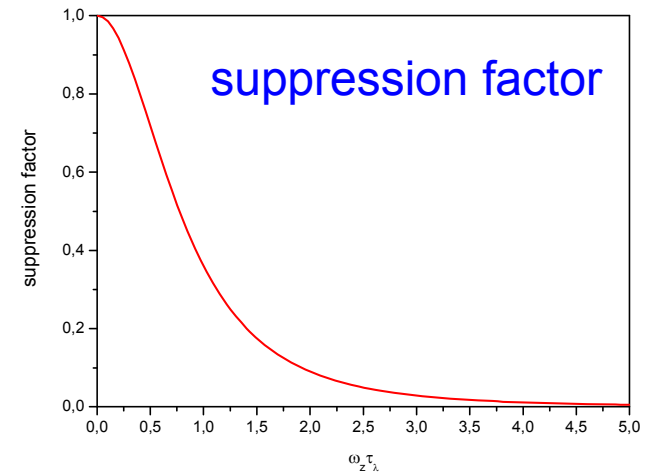
condition of non-adiabaticity: $(\omega_z \tau_\lambda)^2 \ll 1$ $\left(\frac{2\pi\tau_\lambda}{T_{\omega_z}} \ll 1 \right)$

$$\beta = \frac{1}{2} \left[\frac{2\omega_\lambda \tau_\lambda}{1 + (\omega_z \tau_\lambda)^2} \right]^2 \approx 2(\omega_\lambda \tau_\lambda)^2 \quad \text{maximal possible depolarization}$$

condition of adiabaticity: $(\omega_z \tau_\lambda)^2 \gg 1$ $\left(\frac{2\pi\tau_\lambda}{T_{\omega_z}} \gg 1 \right)$

$$\beta = \frac{1}{2} \left[\frac{2\omega_\lambda \tau_\lambda}{1 + (\omega_z \tau_\lambda)^2} \right]^2 \approx 2 \frac{(\omega_\lambda \tau_\lambda)^2}{(\omega_z \tau_\lambda)^4}$$

suppression factor: $\left[\frac{1}{1 + (\omega_z \tau_\lambda)^2} \right]^2$



UCN depolarization after n collisions

$$1) P_1 = P_0 \left(1 - \frac{\varphi^2}{2}\right)$$

$$P_2 = P_1 \left(1 - \frac{\varphi^2}{2}\right)$$

$$P_3 = P_2 \left(1 - \frac{\varphi^2}{2}\right)$$

.....

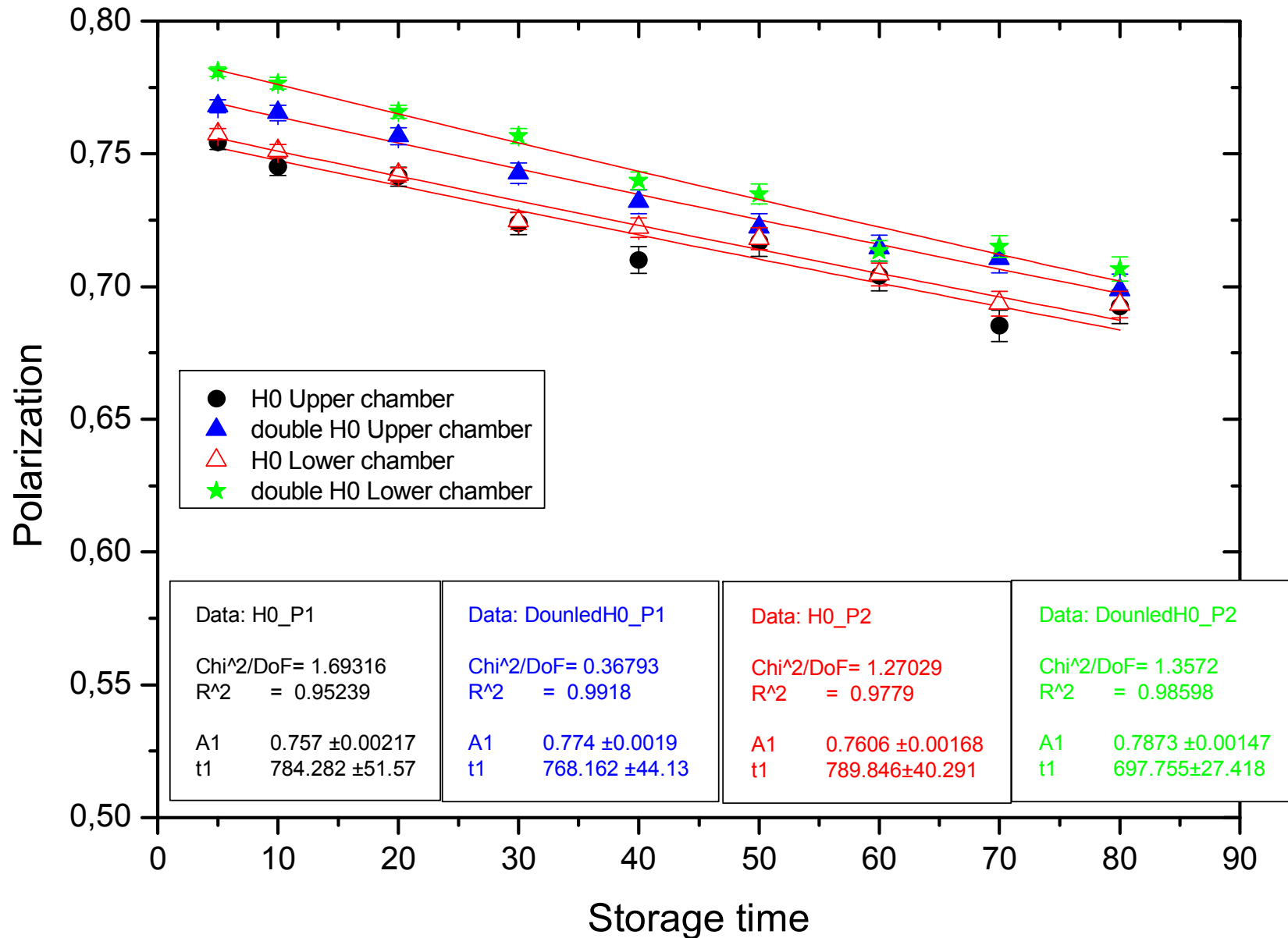
$$P_n = P_0 \left(1 - \frac{\varphi^2}{2}\right)^n \approx P_0 \left(1 - \frac{n\varphi^2}{2}\right) = P_0 \left(1 - \frac{fT\varphi^2}{2}\right)$$

where n – average number of collisions, f – the frequency of collisions with the vertical wall in a unit of time, T – UCN storage time

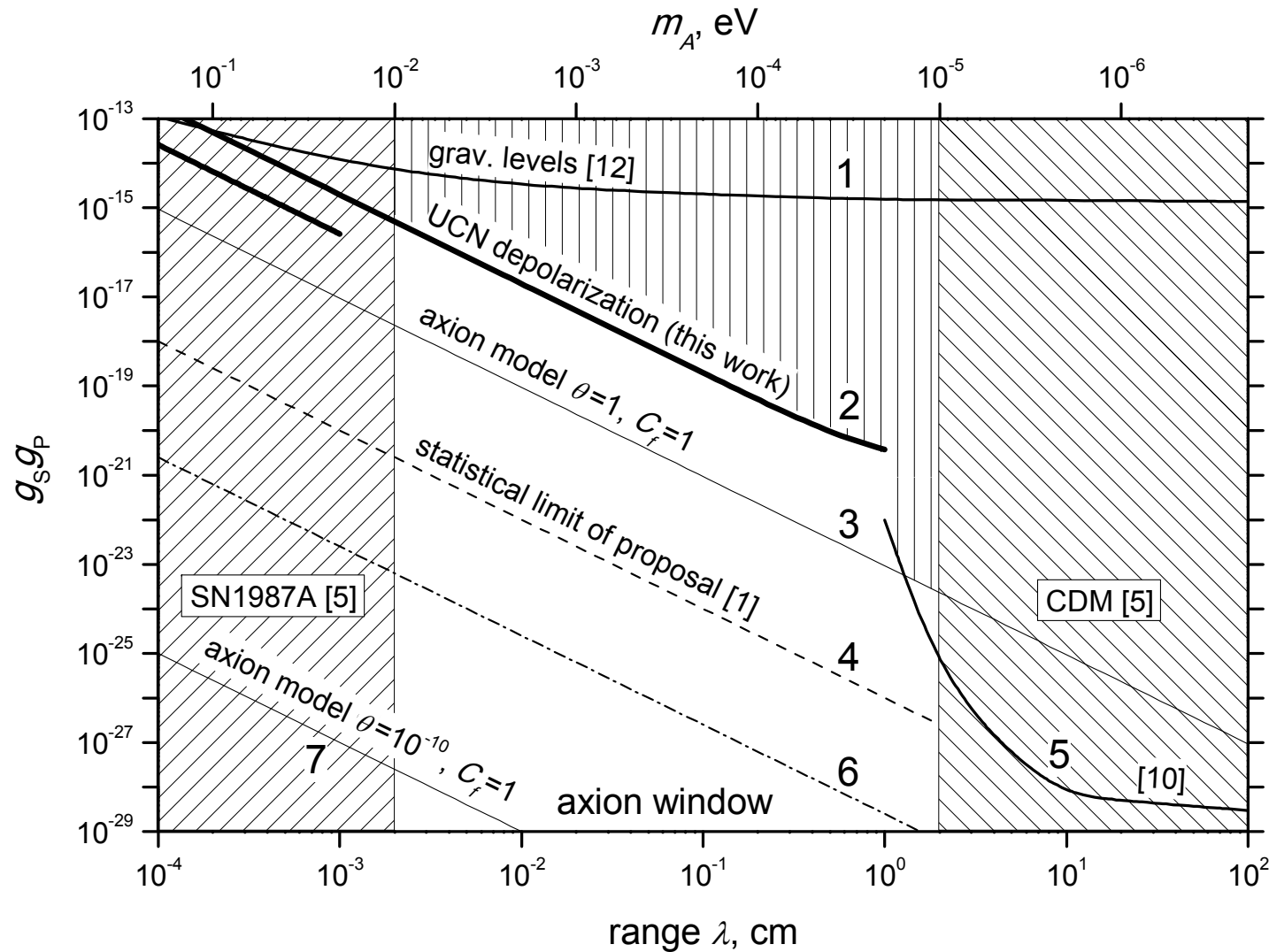
$$2) \varphi_\Sigma = \sqrt{n}\varphi$$

$$P_z = P_0 \left(1 - \frac{\varphi_\Sigma^2}{2}\right) = P_0 \left(1 - \frac{n\varphi^2}{2}\right) = P_0 \left(1 - \frac{fT\varphi^2}{2}\right)$$

Measurement of UCN depolarization in EDM spectrometer



New constraints for CP-violating forces between nucleons in the range 10^{-4} cm \div 1 cm



$$g_S = \frac{C_{p,n} m_{n,p}}{f_A} \theta$$

$$g_P = \frac{C_n m_n}{f_A}$$

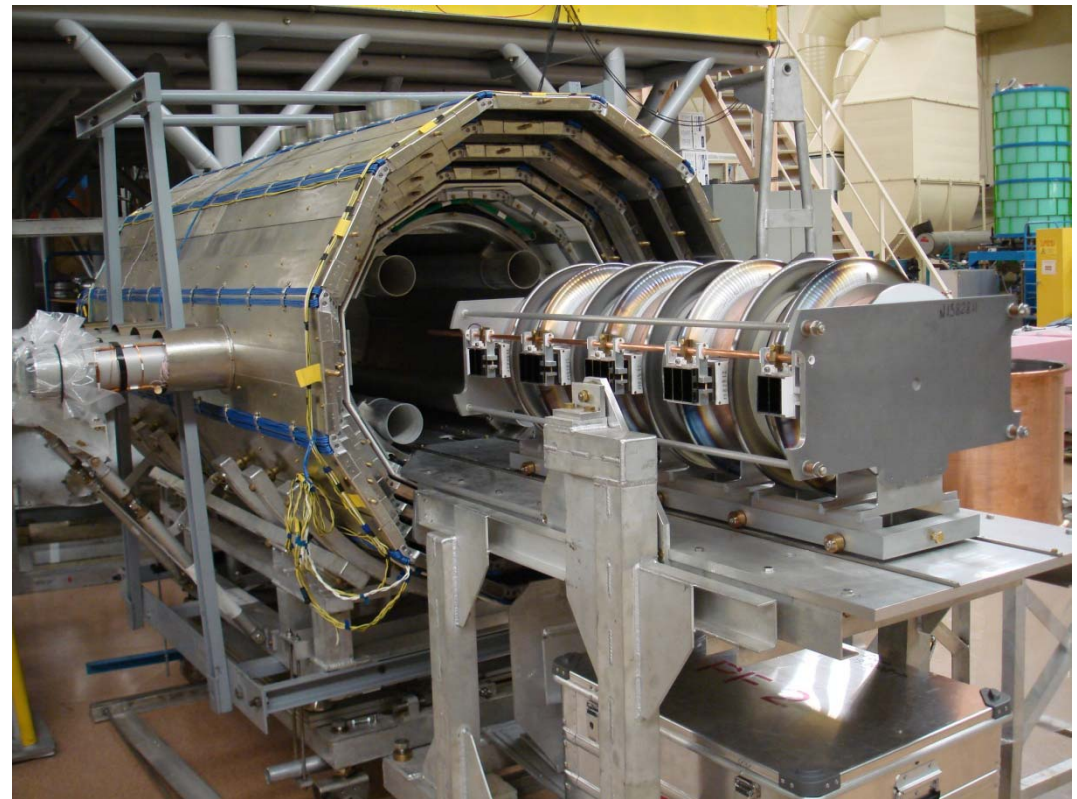
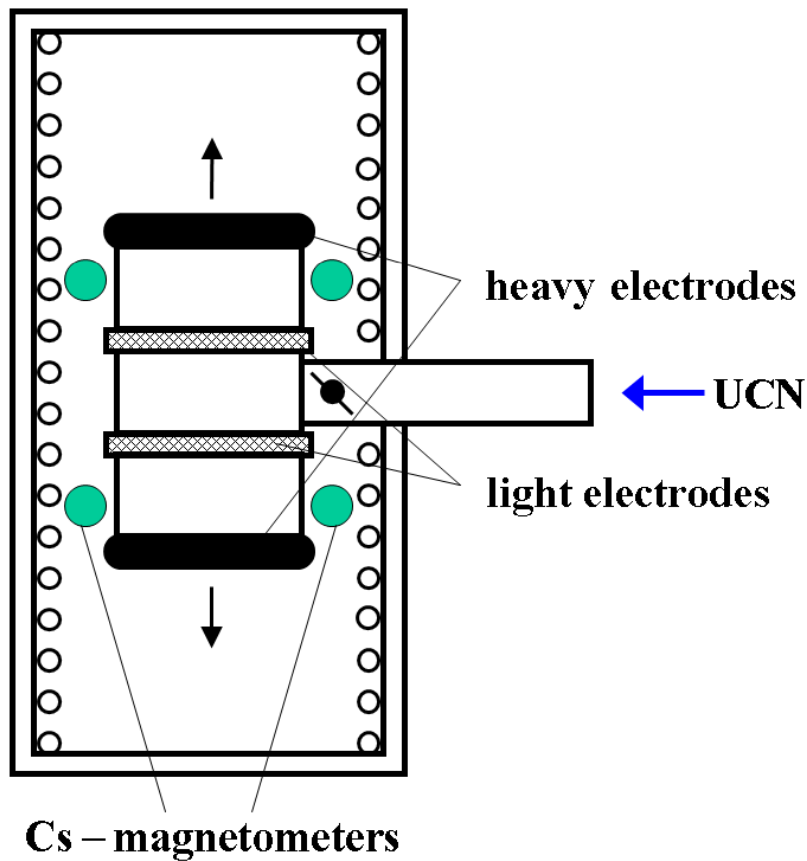
$$m_A = \frac{z^{1/2} f_\pi m_\pi}{1+z} \frac{1}{f_A}$$

$$\lambda_A = \frac{\hbar}{m_A c}$$

$$g_S g_P \lambda^2 \approx 10^{-23} C_f^2 \theta$$

1 – gravitational levels [12]; 2 – UCN depolarization; 3 – axion model with $\theta=1$, $C_f=1$; 4 – statistical limit of resonance shift method [1]; 5 – [10]; 6 – constraints for $g_S g_P$ from independent limits for g_S [15] and g_P [5]; 7 – axion model with $\theta = 10^{-10}$, $C_f=1$.

The future progress in this task is possible by means search for shift of resonance line. For this purpose the multi-chamber EDM spectrometer can be used
(See talk of Oliver Zimmer.)



Final conclusion

Both experimental tasks:

- search for pseudo-magnetic CP-violating field
- search for neutron EDM

should be realized
using different EDM spectrometers